frontiers | Frontiers in Earth Science

TYPE Original Research
PUBLISHED 10 January 2023
DOI 10.3389/feart.2022.1041164

OPEN ACCESS

EDITED BY
Shuai Yin,
Xi'an Shiyou University, China

REVIEWED BY
Yi Ding,
Chengdu University of Technology, China
Meng Wang,
Chongqing University of Science and Technology, China

*CORRESPONDENCE
Zhanlei Wang,
28142547@qq.com

SPECIALTY SECTION
This article was submitted to Structural Geology and Tectonics, a section of the journal Frontiers in Earth Science

RECEIVED 10 September 2022
ACCEPTED 29 September 2022
PUBLISHED 10 January 2023

CITATION
Gu Y, Wang Z, Yang C, Luo M, Jiang Y, Luo X, Zhou L and Wang H (2023), Effects of diagenesis on quality of dengying formation deep dolomite reservoir, Central Sichuan Basin, China: Insights from petrology, geochemistry and in situ U-Pb dating.
Front. Earth Sci. 10:1041164.
doi: 10.3389/feart.2022.1041164

Effects of diagenesis on quality of dengying formation deep dolomite reservoir, Central Sichuan Basin, China: Insights from petrology, geochemistry and *in situ* U-Pb dating

Yifan Gu[1,2], Zhanlei Wang[1,2]*, Changcheng Yang[3], Mingsheng Luo[3], Yuqiang Jiang[1,2], Xiaorong Luo[1,2], Lu Zhou[1,2] and Haijun Wang[1,2]

[1]School of Geoscience and Technology, Southwest Petroleum University, Chengdu, China, [2]The Unconventional Reservoir Evaluation Department, PetroChina Key Laboratory of Unconventional Oil and Gas Resources, Chengdu, China, [3]PetroChina Southwest Oil and Gas Field Company, Chengdu, China

The Ediacaran Dengying Formation in Central Sichuan Basin is the deep dolomite gas reservoir with the largest natural gas reserves in China, providing an excellent example for understanding the effect of diagenesis evolution on deep dolomite reservoir quality. By integrating petrology, geochemistry and *in situ* U-Pb dating, this study aims to reveal the genesis of different rock fabrics and their corresponding diagenetic events, and to discuss the temporal relationship of diagenetic events and their effects on the reservoir quality of Dengying Formation. Two phases of dolomite and three phases of dolomite cement are identified in Ediacaran Dengying Formation deep dolomite reservoirs of Central Sichuan Basin as follows: 1) matrix dolomites (MD), 2) fine-medium crystalline dolomites (FMD), 3) fibrous dolomites (FD), 4) medium-coarse crystalline dolomites (MCD), and 5) saddle dolomite (SD). By analyzing petrographic and temporal relationships between these fabrics, it is suggested that the deep dolomite reservoir of Dengying Formation in Central Sichuan Basin has experienced six diagenetic stages, including 1) syndiagenetic stage, 2) the first-time early diagenetic stage, 3) epidiagenetic stage, 4) the second-time early diagenetic stage, 5) middle diagenetic stage and 6) late diagenetic stage. Microbial dolomitization during syndiagenetic stage produced limited increase in reservoir porosity, but it is of great significance for preservation of reservoir spaces. Silicification is most unfavorable for reservoir formation, but its duration and influence range are very limited. At epidiagenetic stage, the physical properties of Dengying Formation dolomite reservoir have been greatly improved. Two-time early diagenetic stages are both destructive for preservation of reservoir spaces. During middle diagenetic stage, two-stage of hydrothermal alterations occurred, corresponding to Late Silurian to Devonian and Late Permian, respectively. Hydrothermal alteration of the MD is both constructive and

destructive, but overall it is constructive, and the improvement of physical properties is limited. For the karstified MD, both two-stage hydrothermal alterations were destructive, resulting in damage of reservoir physical properties caused by cementation by two-stage SD and one-stage MVT minerals.

KEYWORDS

deep dolomite reservoir, ediacaran dengying formation, diagenetic stage, geochemistry, U-Pb dating, central sichuan basin

1 Introduction

The worldwide exploration practice shows that there are abundant oil and gas resources in dolomite strata (Zhao et al., 2014; Zhao et al., 2018), and remarkable exploration success has been achieved in shallow-middle buried dolomite reservoir (Zou et al., 2011; Jiang et al., 2017; Wang et al., 2018; Gu et al., 2020; Gu et al., 2021). Previous studies have proposed that, affected by destructive diagenesis such as compaction and cementation, with the increase of burial depth and the aging of strata, the porosity in dolomite reservoir gradually decreases, and it is difficult for effective reservoirs to exist in deep buried dolomite strata (Schmoker and Hally, 1982; Ehrenberg et al., 2009). However, in recent years, with the increasing progress of exploration technology, the oil and gas exploration of dolomite reservoirs has gradually advanced to deep strata (buried depth>4500 m) and ultra-deep strata (buried depth >6000 m), and more and more successful examples have been found in Sichuan Basin and Tarim Basin (Guo et al., 2016; Zhao et al., 2021; Li et al., 2022a). Although there have been some successful cases, the exploration and development of deep or ultra-deep dolomite reservoirs still face huge technical and commercial risks. In particular, these dolomite reservoirs are characterized by large burial depth and generally experienced complex diagenetic alteration processes (Du et al., 2018; Peng B. et al., 2018; Gu et al., 2019). Correspondingly, the reservoir rock exhibits extremely complicated characteristics due to the superimposition of multiple diagenetic events (Wang et al., 2014; Xu et al., 2016; Zhu et al., 2019). Therefore, understanding the relationship between different diagenetic stages and corresponding effect on reservoir characteristics is of great significance for the future exploration of deep dolomite reservoir.

At present, the Ediacaran Dengying Formation in the Central Sichuan Basin is the deep dolomite gas reservoir with the largest natural gas reserves in China, and its proven reserves are close to $6 \times 10^{11} m^3$ (Zhao et al., 2021). The abundant drilling cores of the Dengying Formation provide an excellent study target for the effect of diagenesis evolution on the quality of deep dolomite reservoirs. In terms of the reservoir-forming mechanism of deep dolomite reservoirs in the Dengying Formation, most of the viewpoints believe that the supergene karstification during Tongwan Movement plays a key role (Wang et al., 2014; Zhou et al., 2016; Zhou et al., 2020; Su et al., 2022). Zhu et al. (2015) agreed with this view, but also emphasized the constructive role of recrystallization during supergene karstification. After 2013 (Shi et al., 2013; Liu et al., 2014; Peng J. et al., 2018; Gu et al., 2019), scholars have noticed the existence of multi-stage hydrothermal alteration in deep dolomite reservoir of the Dengying Formation and proposed that hydrothermal alteration increases the porosity of the Dengying Formation matrix dolomite by 3%–5% (Liu et al., 2014). However, Jiang et al. (2016) proposed that porosity could only increase by 2% after hydrothermal alteration. In addition to the above viewpoints, some scholars believe that the Dengying large-scale high-quality reservoir is mostly formed in the early sedimentary-diagenetic stage. Although previous studies have obtained these valuable understandings, the temporal relationship between the diagenetic events of the Dengying Formation, the corresponding fluid genesis and its influence on the quality of deep dolomite reservoirs are still unclear.

The purpose of this study is to reveal the genesis of different rock fabrics and corresponding diagenetic events, and to discuss the temporal relationship of diagenetic events and their effects on the reservoir quality. The results of this study not only provide an in-depth understanding of the genetic mechanism of deep ancient dolomite reservoirs, but also provide a scientific basis for future exploration of the Ediacaran Dengying Formation in Sichuan Basin.

2 Geological background

The Sichuan Basin, situated in the northwest region of the Upper Yangtze platform (Ding et al., 2021) (Figure 1A), is the most petroliferous basin for oil and gas exploration of unconventional reservoir in China (He et al., 2021; Zhou et al., 2021; Li H. et al., 2022; Li et al., 2022b; Li, 2022). The study area is located in the Central Sichuan Basin. In this area, the Ediacaran Dengying Formation and the underlying Doushantuo Formation are in conformable contact, but is in unconformable contact with the overlying mudstone (or shale) of the Lower Cambrian Qiongzhusi Formation. According to rock type, microbial content and sedimentary structure, the Dengying Formation can be divided into four members from bottom to top. The first, second and fourth members are all composed of

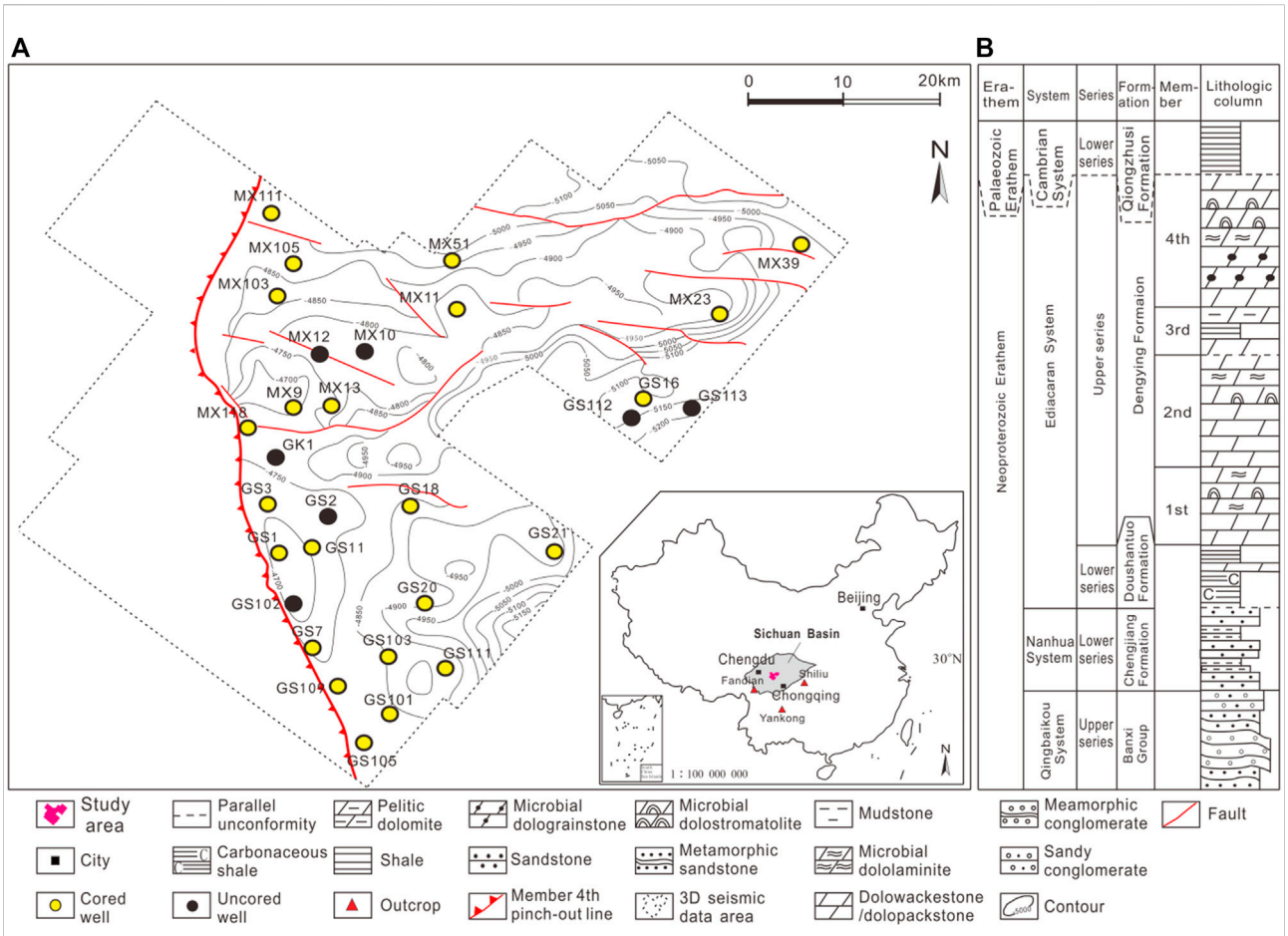

FIGURE 1
(A) The spatial distribution map showing the study area and drilling wells in the Central Sichuan Basin. **(B)** Generalized stratigraphy of the Ediacaran Dengying Formation in the study area (modified from Gu et al., 2019).

dolomite, except for the third member composed of mudstone and argillaceous dolomite (Jiang et al., 2016). The matrix dolomite (MD) consists of microbial dololaminite, microbial dolostromatolite, dolowackestone and dolopackstone (Figure 1B).

3 Samples and methods

At first, 157 samples from drilling cores of the Dengying Formation were doubly polished, followed by blue epoxy-impregnation and staining with Alizarin red for identification of different rock fabrics. And then petrographic relationships of different fabrics were delineated using a CL8200MK5 cathodoluminescence (CL) microscope. Eighteen samples were selected for Sr isotope measurement through a Finnigan Triton thermal ionization mass spectrometer (TIMS). Eighty-four samples were selected for stable isotopic ($\delta^{18}O$, $\delta^{13}C$) measurement using MAT253 isotope mass spectrometer. The $\delta^{18}O$ and $\delta^{13}C$ data are normalized to Vienna Pee Dee Belemnite (V-PDB) standard and corrected by fractionation factors proposed by Fairchild and Spiro (1987). Twenty-seven samples were selected for rare earth element (REE) contents measurement through inductively coupled plasma-mass spectrometry (ICP-MS) at Sichuan Origin & Microspectrum Corporation. Firstly, the 27 samples were dissolved by hydrofluoric acid and nitric acid in a closed container. The hydrofluoric acid were wiped out by evaporation on the electric heating plate, and then dissolved by nitric acid. After dilution, the samples are directly measured by ICP-MS. The analytical uncertainties are estimated to be 5%. Standard rock reference material (GSD-9) were used to monitor the analytical accuracy and precision.

Laser *in situ* U-Pb isotopic dating was carried out through LA-ICP-MS (Element XR) at Sichuan Origin & Microspectrum Corporation in Chengdu. For the dolomite samples selected for dating, spots with higher ^{238}U intensities, higher $^{238}U/^{206}Pb$ ratios and lower $^{207}Pb/^{206}Pb$ ratios were selected for further U-Pb isotope analysis. Additional spots may be selected from the

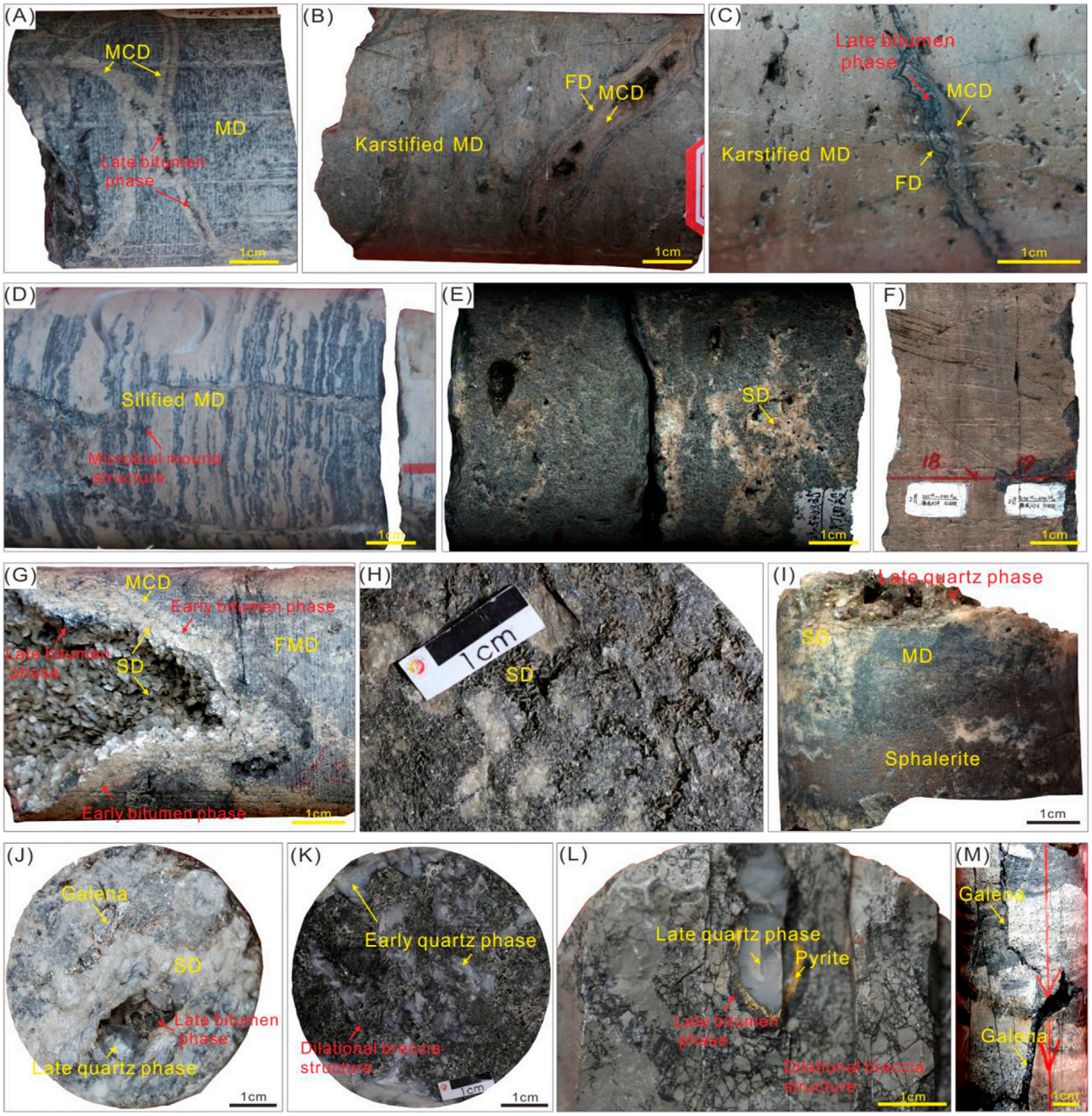

FIGURE 2
Macroscopic characteristics for the Dengying Formation from drilling cores in Central Sichuan Basin. **(A)** MCD and late bitumen phase filled in fractures within the MD, Well GS20, 4th Member, 5187.57 m. **(B)** FD and MCD filled in vugs within karstified MD, Well GS102, 4th Member, 5085.11 m–5085.36 m. **(C)** The original sedimentary structures in the MD have almost disappeared, Well GS7, 4th Member, 5266.49 m–5266.59 m. **(D)** The original microbial mound structures are well preserved in silified MD, Well GS18, 4th Member, 5184.13 m. **(E)** Scattered intercrystalline pores within FMD, Well GS16, 4th Member, 5453.35 m. **(F)** Scattered intercrystalline pores within FMD, Well MX103, 4th Member, 5195.24 m. **(G)** MCD, early bitumen phase and saddle dolomite (SD) coats inner wall of hydrothermal dissolved vug within FMD, Well GS20, 4th Member, 5195.7 m **(H)** SD with curved or lobate crystal faces filled between dilational breccias, Well MX51, 4th Member, 5335.7 m **(I)** SD, sphalerite and late quartz phase filled in vugs within karstified MD, Well GS102, 4th Member, 5043.93 m. **(J)** Mississippi Valley-Type minerals including galena and late quartz phase, Well GS109, 4th Member, 5316.08 m. **(K)** Early quartz phase filled between dilational breccias, Well MX51, 4th Member, 5401.77 m. **(L)** Pyrite and late quartz phase filled in vugs within dilational breccia structure, Well MX39, 4th Member, 5309.3 m. **(M)** Galena filled in fractures within MD, Well GS101, 4th Member, 5517.2 m.

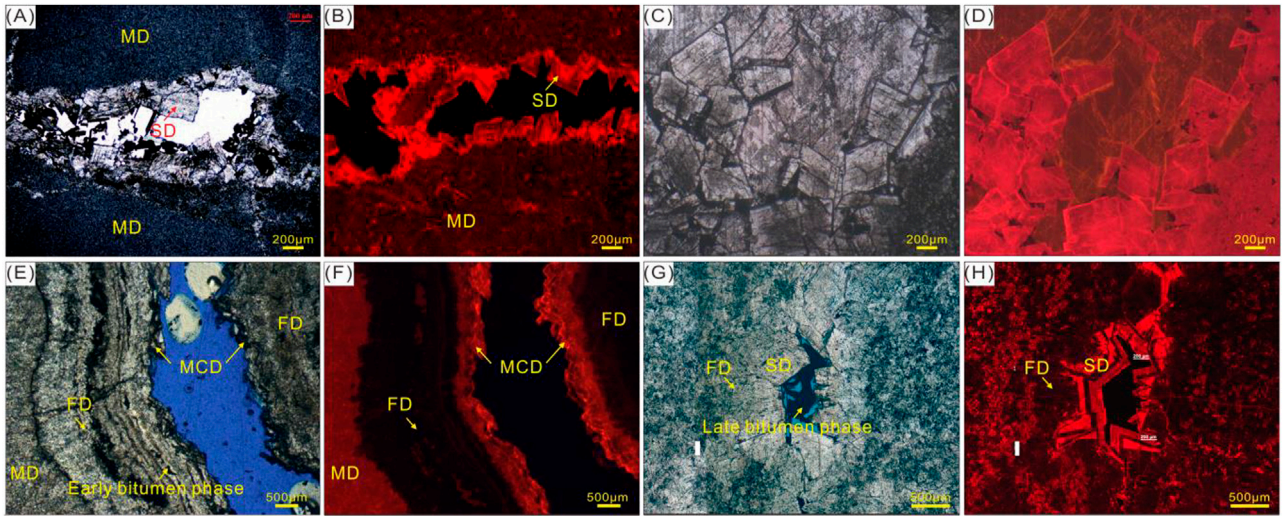

FIGURE 3
Microscopic characteristics for the Dengying Formation from drilling cores in Central Sichuan Basin. **(A)** SD along vug interwall within MD under PPL, Well GS1, 4th Member, 4970 m (Gu et al., 2019). **(B)** SD exhibits bright red and banded structure whereas MD exhibit dull red under CL, Well GS1, 4th Member, 4972 m. **(C)** FMD with cloudy core and clear rim, Well GS16, 4th Member, 5450.15 m. **(D)** FMD exhibits bright red under CL, Well GS16, 4th Member, 5450.15 m. **(E,F)** FD shows nonluminescent and MCD exhibit bright red under CL, Well GS102, 4th Member, 5079.65 m. **(G,H)** FD shows non-luminescent, and SD exhibit bright red and banded structure under CL, Well GS16, 4th Member, 5462 m.

vicinity of those pre-screened spots with the highest $^{238}U/^{206}Pb$ ratios, so that sufficient U-Pb isotope spot analyses can be obtained for each sample. We use laser spot size of 160 um in diameter, laser energy of 3 J/cm^2 and repetition rate of 10 Hz. The measurement cycle comprised a cleaning sequence of 20 shots, a preablation background of 15 s, an ablation period of 25 s and a washout time of 8 s. The duty cycle included only ^{206}Pb, ^{208}Pb, ^{232}Th, and ^{238}U. The samples were measured together with NIST-614 glass standard and several matrix-matched laboratory working calcite standards, such as WC-1. Repeated measurements of the NIST-614 glass standard bracketing the unknown samples and calcite standards were used to correct for $^{207}Pb/^{206}Pb$ fractionation and for instrument-related drift in the $^{206}Pb/^{238}U$ ratios. WC-1 calcite standard independently dated to 254.4 ± 6.4 Ma (Roberts et al., 2017) was also dated together with the dolomite samples as the control standard to ensure reproducibility, which gave results within 2% of the reference value among different sessions.

4 Results

4.1 Petrological characteristics

4.1.1 Dolomite phases

4.1.1.1 *Matrix dolomites (MD)*

Microscopically, the crystal size of the MD is usually less than 50 μm (Gu et al., 2019). Without constructive diagenesis, the reservoir space of MD is hardly developed due to tiny crystal size (Figure 3A). After alteration by dissolution, large numbers of pores or vugs are formed within MD (Figures 2A,B), and the original sedimentary structures of MD have almost disappeared (Figure 2C). But after early-stage silicification, the silicified MD becomes extremely dense and less susceptible to other diagenesis (Figure 2D). Under CL, the MD is nonluminescent (Figure 3B).

4.1.1.2 *Fine-medium crystalline dolomites (FMD)*

The FMD has a crystal size of 200–450 μm (Gu et al., 2019), most of which is characterized by a nonplanar anhedral or planar subhedral texture with cloudy cores and clean rims (Figure 3C). A large number of scattered intercrystalline pores have developed between crystals filled with bitumen (Figures 2E,F). Under cross-polarized light, the FMD shows typical patterns of wavy extinction (Gu et al., 2019). Under CL, the FMD is bright red with a zonal texture (Figure 3D).

4.1.2 Dolomite cement phases

4.1.2.1 *Fibrous dolomites (FD)*

The FD is present as an isopachous fibrous dolomite coating vug internal walls (Figures 3E,F), which is commonly distributed between larger saddle dolomite (or medium-coarse crystalline dolomite) crystals and host-rock (Figure 3G). In terms of CL color, crystal habit, and size, the FD exhibit obvious difference from saddle dolomite (Figure 3H). The FD under CL is nonluminescent (Figure 3F) and mainly consists of fibrous dolomite with 500 μm in size (Figure 3H) which is clearly

darker than saddle dolomite in transmitted light (Figure 3G). Locally, a fine, dark bitumen line is observed separating FD and saddle dolomite cements (Figure 3E).

4.1.2.2 *Medium-coarse crystalline dolomites (MCD)*

The MCD cements predominantly coat vugs or fractures, showing a sharp contact with the host MD (Figure 3E). The MCD primarily comprises of clear, coarse dolomite crystals growing along internal walls of reservoir spaces, with a bright red luminescence under CL (Figure 3F). A dark bitumen line is ubiquitously present between MCD and saddle dolomite cements (Figure 2G), suggesting an oil emplacement episode predating saddle dolomite cements.

4.1.2.3 *Saddle dolomites (SD)*

Saddle dolomite is the most common dolomite cement in cores and thin sections of the Dengying Formation (Figures 2G,H). Macroscopically, the SD is characterized by curved crystal faces and grayish white in color (Figures 2H,I). In some core samples, the SD coexist with MVT minerals such as sphalerite, galena, and quartz (Figures 2I,J). Under CL, the SD is characterized by alternating luminescence between bright red and dark red (Figures 3G,H).

4.2 Mississippi valley-type (MVT) minerals

MVT Pb-Zn mineral assemblages were occasionally found in pores, vugs, and fractures of the host-rock MD (Figure 2J), but they are relatively low in abundance on the whole. Brownish red sphalerite (Figure 2I), glassy (or gray-white) quartz (Figures 2J,K), golden yellow pyrite (Figure 2L) and silver-white galena mainly occur as fracture- and/or vug-filling minerals (Figure 2M).

4.3 Geochemistry and fluid inclusion

4.3.1 Oxygen, carbon, and strontium isotopes

According to data from previous studies and this study (Zhou et al., 2016; Feng et al., 2017; Peng B. et al., 2018; Gu et al., 2019; Zhou et al., 2020; Su et al., 2022), the MD yields $\delta^{18}O$ values varying from −7.80‰ to + 0.89‰V-PDB (average −4.17‰V-PDB, n=51) and $\delta^{13}C$ values of −0.46‰ to + 7.14‰V-PDB (average + 2.66‰V-PDB, n=51). The FD yields $\delta^{18}O$ values varying from −4.34 to −1.25‰V-PDB (average −3.02‰V-PDB, n=14) and $\delta^{13}C$ values of + 1.12‰ to + 5.36‰V-PDB (average + 2.80‰V-PDB, n=14). The FMD yields $\delta^{18}O$ values varying from −13.84‰ to −4.94‰V-PDB (average −8.37‰V-PDB, n=33) and $\delta^{13}C$ values of −1.93‰ to + 5.29‰V-PDB (average + 1.69‰V-PDB, n=33). The MCD yields $\delta^{18}O$ values varying from −13.32‰ to −8.70‰V-PDB (average −11.32‰V-PDB, n=22) and $\delta^{13}C$ values of −0.32‰ to + 4.96‰V-PDB (average + 2.09‰V-PDB, n=22). The SD yields $\delta^{18}O$ values varying from −14.76‰ to −6.80‰V-PDB (average −12.11‰V-PDB, n=21) and $\delta^{13}C$ values of −5.43‰ to + 2.94‰V-PDB (average −1.20 ‰VPDB, n=21) (Figure 4A).

The MD has $^{87}Sr/^{86}Sr$ ratios ranging from 0.707789 to 0.709800 (average 0.708804, n=10) (Zhou et al., 2016; Feng et al., 2017; Gu et al., 2019; Su et al., 2022). The $^{87}Sr/^{86}Sr$

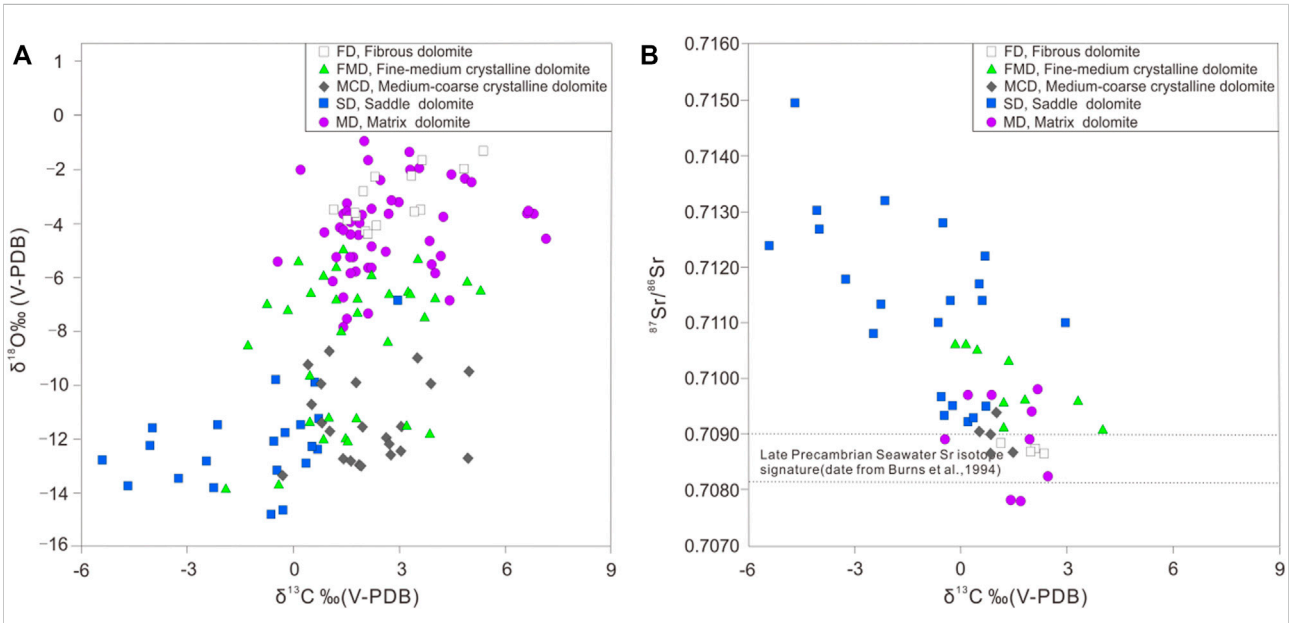

FIGURE 4
(A) Crossplot of $\delta^{13}C$ and $\delta^{18}O$ for different rock fabrics in the Dengying Formation of Central Sichuan Basin (FD, MCD, and SD data are from Feng et al., 2017; Su et al., 2022). **(B)** Crossplot of $\delta^{13}C$ and $^{87}Sr/^{86}Sr$ for different rock fabrics in the Dengying Formation of Central Sichuan Basin ($^{87}Sr/^{86}Sr$ data for FD, MCD, and SD are from Feng et al., 2017; Su et al., 2022; $^{87}Sr/^{86}Sr$ data for late Precambrian seawater are from Burns et al., 1994).

ratios of the FD and MCD have a narrow distribution (Figure 4B), ranging from 0.708645 to 0.708832 and 0.708703 to 0.709359, respectively (Su et al., 2022). The FMD has $^{87}Sr/^{86}Sr$ ratios ranging from 0.709060 to 0.710600 (average 0.709877, n=9) (Zhou et al., 2016; Feng et al., 2017). The $^{87}Sr/^{86}Sr$ ratios of the SD has a wide distribution (Figure 4B), ranging from 0.709218 to 0.714959 (average 0.711343, n=21) (Feng et al., 2017; Gu et al., 2019; Su et al., 2022).

4.4 Rare earth elements (REEs)

The distribution patterns of REEs are widely applied as indicators reflecting origin of diagenetic fluid such as dolomitization fluids (Du et al., 2018; Gu et al., 2019). For example, positive Eu anomalies are often used to indicate the occurrence of hydrothermal activities (Gu et al., 2019; Qi et al., 2021; Su et al., 2022). REE+Y data shown as Post-Archaean Australian Shale (PAAS)-normalized diagrams (Shahida et al., 2013) for different dolomite fabrics are shown in Figure 5. The REE+Y patterns for the MD are characterized by slightly Ce negative anomalies, and slightly Eu positive anomalies (Figure 5A). The REE+Y patterns for the silicified MD are characterized by strongly Ce negative anomalies (Figure 5B). The REE+Y patterns for the FD are characterized by slightly Ce negative anomalies (Figure 5C). The MCD shares similar REE+Y patterns with the MD (Figure 5D). The REE+Y patterns for the FMD are characterized by Ce negative anomalies and strongly Eu

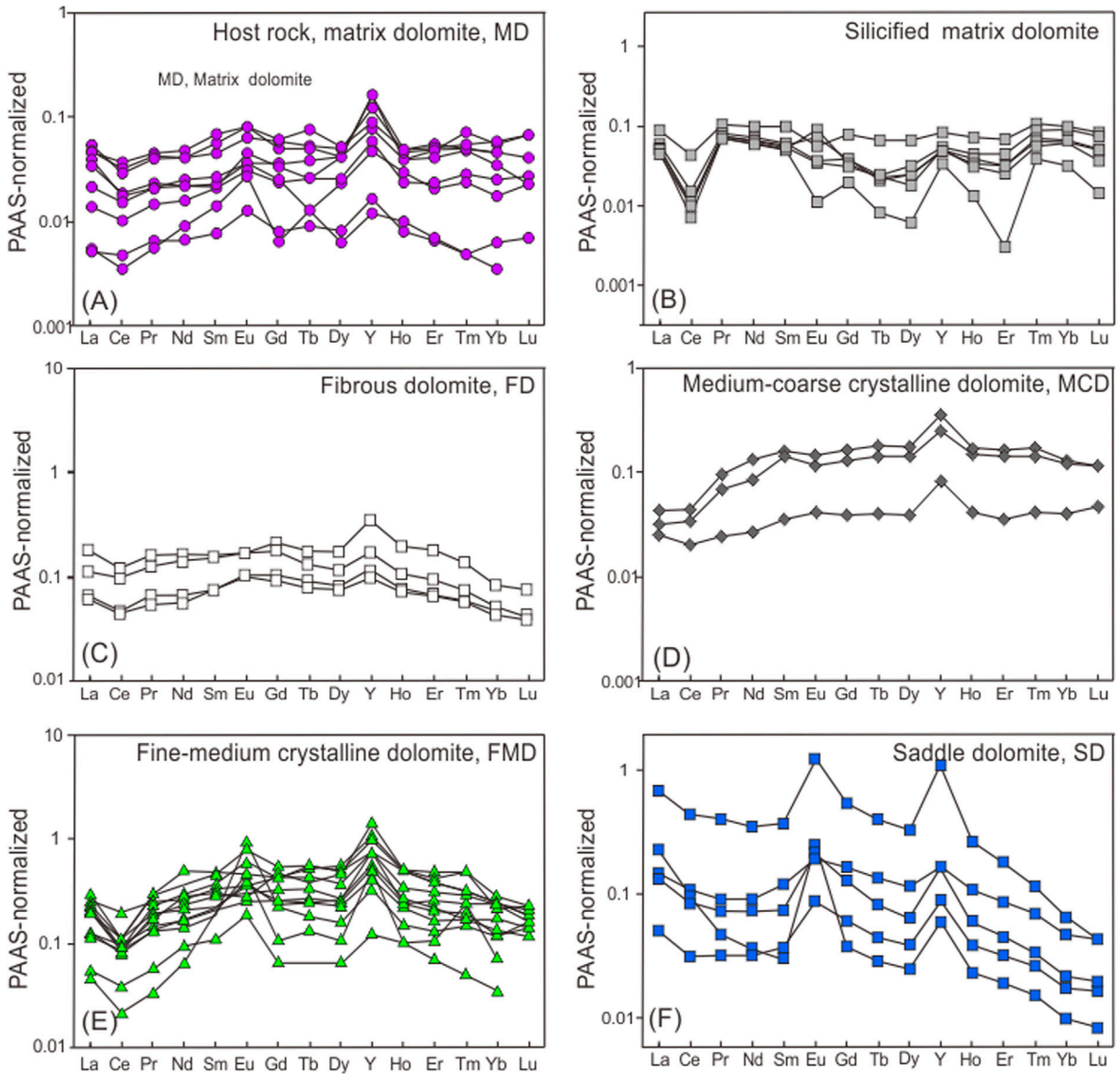

FIGURE 5
REE + Y distribution patterns for different rock fabrics in the Dengying Formation of Central Sichuan Basin (FD and SD data are from Su et al., 2022).

positive anomalies (Figure 5E). The REE+Y patterns for the SD are characterized by strongly Eu positive anomalies (Figure 5F).

4.5 Fluid inclusions

The results of fluid-inclusion petrography and microthermometry for different rock fabrics are displayed in Figure 6. The measurement focuses on primary and pseudo-secondary aqueous inclusions within the dolomite fabrics and quartz cement. Notably, the FD and MD crystals are not suitable for homogenization temperature (Th) measurement owing to its tiny crystal size.

The isopachous FD was formed in a subaerial or submarine environment, suggesting a relatively low precipitation temperature (Ding et al., 2019). Although associated fluid inclusion Th could not be determined, both Th of primary fluid inclusions within Ediacaran halites in the study area and silicon-oxygen isotopes of cherts consistently record Ediacaran seawater temperatures ranging between 13°C and 40°C (Meng et al., 2011). The Th distribution for the MCD range from 77.2°C to 92.8°C, suggesting relatively low-temperature of corresponding diagenetic fluids (Figure 6A). The FMD has Th value in the range between 101.4°C and 152.0°C. The SD has two temperature ranges of 116.5°C–183.0°C and 191.2°C–250.3°C, suggesting two episodes of hydrothermal fluids (Figure 6B). The Th distribution of quartz is similar to that of SD, and it also has two temperature ranges, 115.5°C–162.3°C and 198.6°C–227.2°C, respectively. It is suggested that the two stages of quartz phases were precipitated from two different episodes of hydrothermal fluids.

5 Discussion

5.1 Origin and formation timing of dolomite phases

5.1.1 Matrix dolomite (MD)

Although the dolomitization mechanism of the Ediacaran Dengying Formation is still controversial, we agree with the views that dolomitization of the Dengying Formation occurs in the syndiagenetic stage in terms of well-preserved microbial structure (Peng J. et al., 2018; Zhou et al., 2020). To better understand this unique dolomitization mechanism, a few studies illustrate that microorganisms survived and reproduced in shallow water platforms. After death, they deposited together with carbonate sediments. When the microbial-rich carbonate sediments are below the sediment-water interface, the water body changes from an oxidizing condition to a reducing condition. The organic matter in the microorganism began to decompose under the action of sulfate-reducing bacteria, which decreased sulfate in the seawater to overcome the kinetic barriers of dolomite precipitation and accelerated this process (Zhou et al., 2020).

5.1.2 Fine-medium crystalline dolomites (FMD)

Petrological relationships indicate that the FMD is the part of the MD in which the dolomite crystals become larger after recrystallization (Figure 2E). Compared to MD, the FMD has a more negative $\delta^{18}O$ and a higher $^{87}Sr/^{86}Sr$ ratios, and the FMD isotope data points are concentrated between MD range and SD range (Figure 4). The REE+Y distribution patterns of the FMD also has the characteristics of MD and SD. The above geochemical characteristics confirm the close affinity between FMD and MD, SD (Figure 5). Based on Th measurement results, the Th distribution of the FMD is more close to early SD phase (Figure 6). The U-Pb ages of the two first-stage SD samples measured in this study are 408 ± 40 Ma and 403 ± 30 Ma, respectively (Figure 7). Combined with the burial history curve (Liu et al., 2018a; Su et al., 2022), it is suggested that the Dengying Formation is in the middle diagenetic stage at this time (Figure 8), so the FMD is the product of the recrystallization of MD caused by the first hydrothermal fluid during middle diagenetic stage.

5.2 Origin and formation timing of dolomite cement phases

5.2.1 Fibrous dolomites (FD)

Petrological relationships indicate that the FD is the earliest cement coating the inner walls of vugs formed in the epidiagenetic stage. The U-Pb age of the FD is 553.6 ± 6.4 Ma, suggesting the FD precipitate during the Tongwan Movement in the epidiagenetic stage (Su et al., 2022). There has long been controversy regarding the parent fluids (freshwater or seawater) that led to the precipitation of FD (Tang et al., 1980; Wang et al., 2014; Lin et al., 2018). The FD is nonluminescent under CL (Figure 3), suggesting oxidizing parent fluids (Dorobek, 1987). The REE+Y distribution patterns of FD and MD have the same characteristics, and the $^{87}Sr/^{86}Sr$ ratios of FD are in the range of coeval seawater (Figure 4). Integrated with latest studies (Peng B. et al., 2018; Peng J. et al., 2018; Ding et al., 2019), it is suggested that the formation of the FD is derived from marine flooding of the karst system during epidiagenetic stage.

5.2.2 Medium-coarse crystalline dolomites (MCD)

Petrological relationship shows that the MCD precipitated later than the FD, but earlier than the early bitumen phase. The U-Pb ages of three MCD samples in this study are very close, which are 513 ± 11 Ma, 510 ± 31 Ma and 520 ± 11 Ma, respectively (Figure 7). Combined with the burial history curve (Liu et al., 2018a; Su et al., 2022), it is illustrated that MCD was formed in the second-time early diagenetic stage of the Dengying Formation.

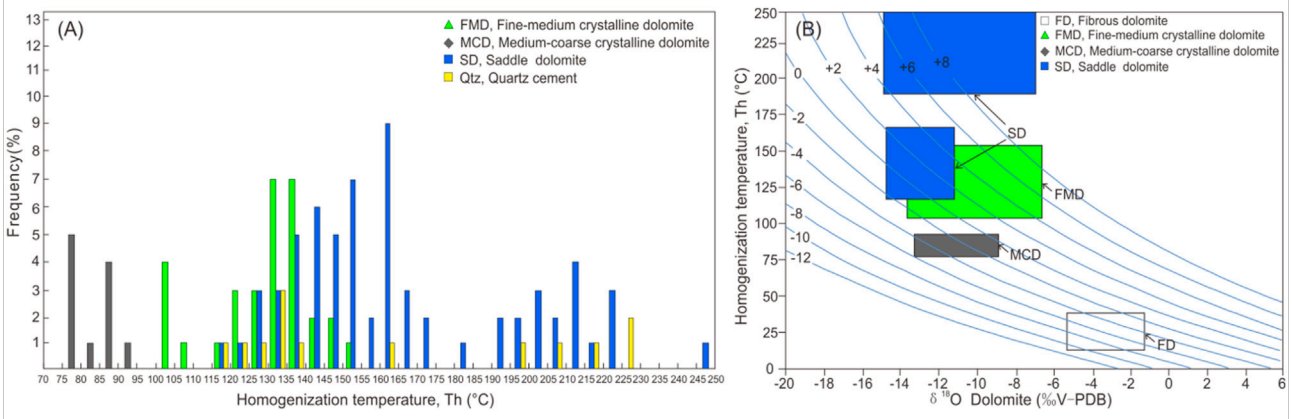

FIGURE 6
(A) Homogenization temperature (Th) distribution of fluid inclusions for different rock fabrics in the Dengying Formation of Central Sichuan Basin and surrounding area (all the Th data are from Feng et al., 2017; Peng J. et al., 2018; Gu et al., 2019; Zhou et al., 2020; Su et al., 2022). **(B)** Crossplot of $\delta^{18}O$ and precipitation temperature for different dolomite fabrics in the Dengying Formation of Central Sichuan Basin and surrounding area (all the Th data are from Feng et al., 2017; Peng B. et al., 2018; Gu et al., 2019; Zhou et al., 2020; Su et al., 2022). The $\delta^{18}O$ (V-SMOW) of dolomite parent fluids was calculated using the equation proposed by Land (1983).

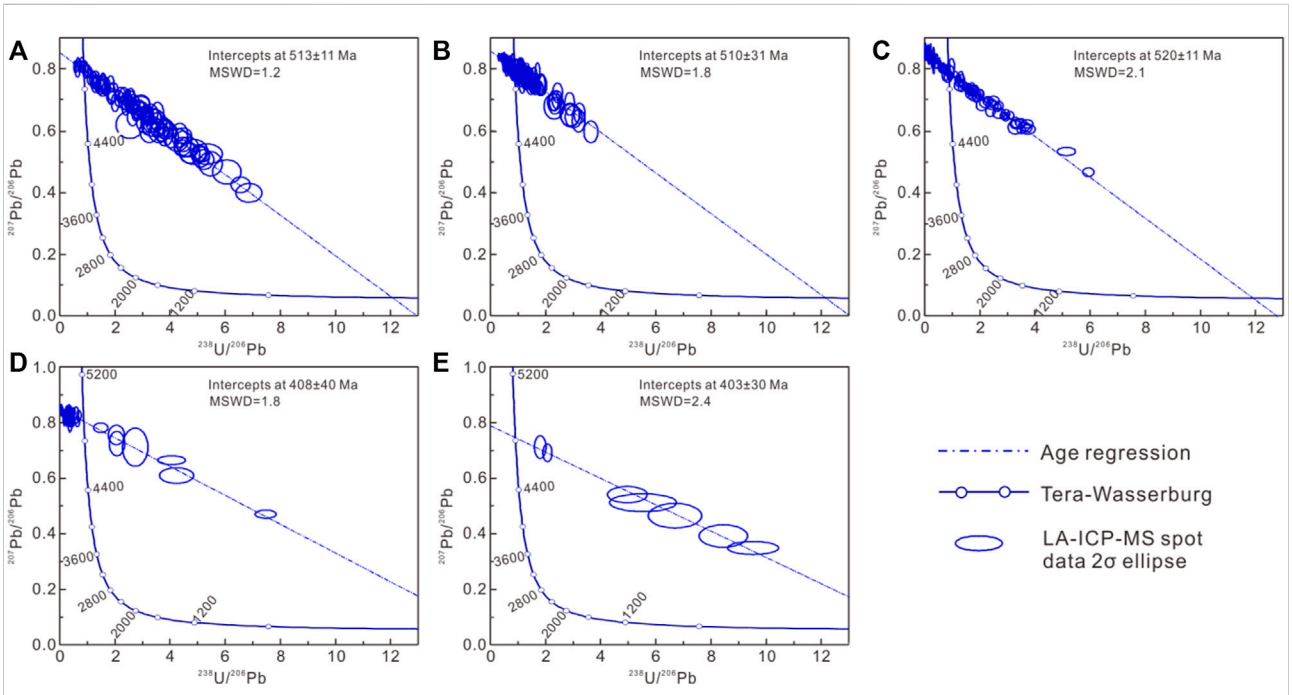

FIGURE 7
(A–C) Tera-Wasserburg Concordia plots showing $^{238}U/^{206}Pb$ vs. $^{207}Pb/^{206}Pb$ of medium-coarse crystalline dolomite (MCD) cement phase in the Dengying Formation of Central Sichuan Basin. **(D,E)** Tera-Wasserburg Concordia plots showing $^{238}U/^{206}Pb$ vs. $^{207}Pb/^{206}Pb$ of early saddle dolomite (SD) cement phase in the Dengying Formation of Central Sichuan Basin.

The REE+Y distribution patterns of MCD does not have Eu positive anomaly, suggesting non-hydrothermal origin (Figure 5). At the same time, its Th is also within the normal range of the early diagenetic stage and is not significantly higher than ambient temperature. Moreover, the $^{87}Sr/^{86}Sr$ ratios of MCD is very closed to coeval seawater and generally similar to host MD record, suggesting that the parent fluids of MCD probably modified coeval seawater.

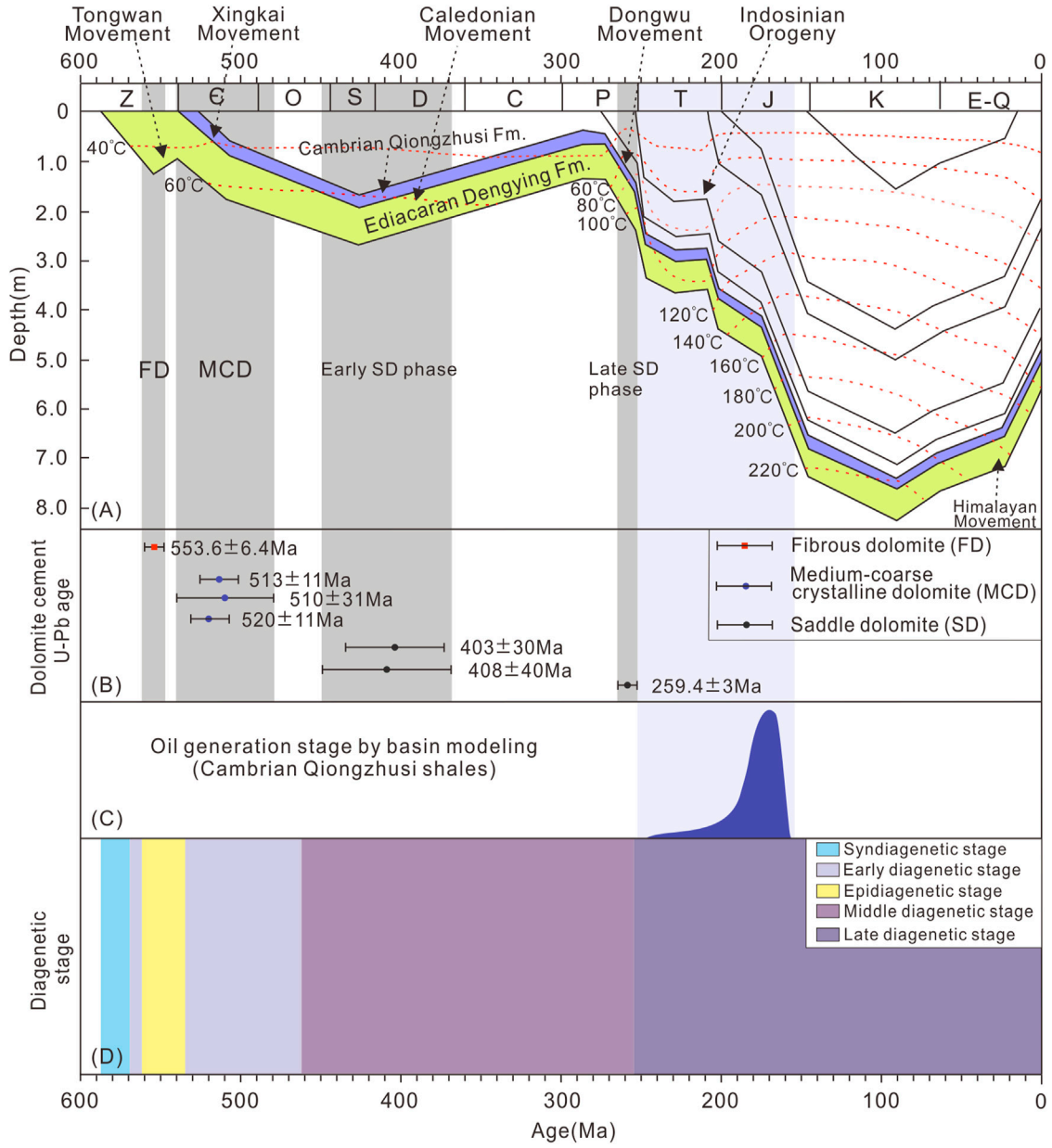

FIGURE 8
(A) Burial-thermal-tectonic evolution history in the Central Sichuan Basin (modified from Liu et al., 2018a; Su et al., 2022). **(B)** *In situ* U-Pb ages for different dolomite cements of the Dengying Formation in the Central Sichuan Basin (data of FD and late SD phase are from Su et al., 2022). **(C)** Oil generation stage of the Cambrian Qiongzhusi shales by basin modeling (Liu et al., 2018b). **(D)** Diagenetic stage of the Dengying Formation in the Central Sichuan Basin.

5.2.3 Saddle dolomites (SD)

The Th measurement results show that the formation of SD can be clearly divided into two episodes (Figure 6), suggesting two episodes of hydrothermal activities. Previous studies have also suggested that there were two-stage hydrothermal activities in the Dengying Formation in the Sichuan Basin, namely, the Late Ediacaran-Early Cambrian and the Late Devonian-Middle Triassic (Liu et al., 2014). Some studies suggest that the second-stage should be limited to the Late Devonian-Late Permian (Jiang et al., 2016; Peng B. et al., 2018). U-Pb dating shows that the early SD phase was precipitated during the Late Silurian to Devonian (Figure 7), when the Dengying Formation was in the middle diagenetic stage. This study did not obtain the U-Pb age of the late SD phase, but Su et al. (2022) determined the U-Pb age of 259.4 ± 3 Ma, this time interval

matches the Late Permian hydrothermal activity triggered by eruption of Emeishan flood basalts (from 257.22 ± 0.37 Ma to 260.55 ± 0.07 Ma) (Huang et al., 2022). Because the Caledonian movement caused the Dengying Formation to be uplifted in the Devonian-Carboniferous and then subsided gradually, the Dengying Formation was still in the middle diagenetic stage in the Late Permian (Figure 8).

5.2.4 Origin of mississippi valley-type (MVT) minerals

Previous studies have noticed the MVT minerals in the Dengying Formation. In view of its coexistence with SD, its hydrothermal origin can be determined (Figure 2). The petrological relationship shows that MVT minerals such as galena, sphalerite, and pyrite coexist with the late quartz phase (Figures 2J–L), indicating that MVT minerals are precipitated from the second-episode hydrothermal fluid. Thus MVT minerals were formed in the Late Permian, when the Dengying Formation was undergoing the middle diagenetic stage.

5.3 Controlling factors and porosity evolution of reservoir

When the Dengying Formation was in syndiagenetic stage for the first time, there were a large number of primary reservoir spaces within microbial sedimentary structures. During

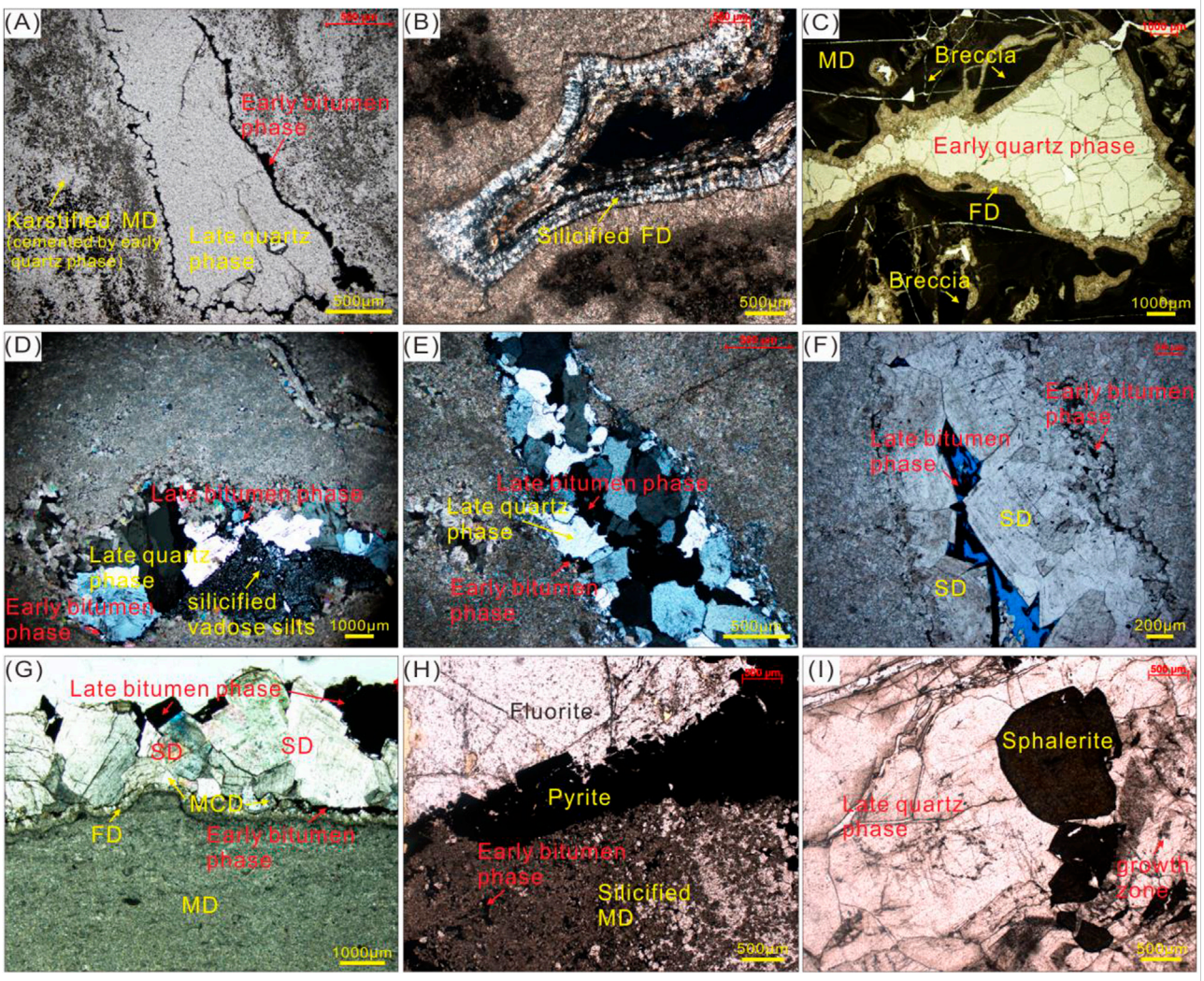

FIGURE 9
Microscopic characteristics of petrographic relationships between different rock fabrics in the Dengying Formation of Central Sichuan Basin. **(A)** Karstified MD cemented by early quartz phase under PPL, Well GS18, 5184.13 m–5184.72 m. **(B)** Silified fibrous dolomites (FD) along inner wall of vugs exhibit grayish white under XPL, Well GS102, 5094.66 m. **(C)** Fibrous dolomites (FD) predating early quartz phase filled along inner wall of vugs formed in epidiagenetic stage, Well MX108, 5304.5 m. **(D)** Vadose silts formed during epidiagenetic stage are silicified by hydrothermal fliuds, Well GS102, 5045.53 m. **(E)** Late quartz phase between two-stage bitumen phase, Well GS102, 5102.89 m. **(F)** Saddle dolomite (SD) between two-stage bitumen phase, Well GS1, 4985 m (Jiang et al., 2016). **(G)** Saddle dolomite (SD) predating fibrous dolomites (FD) and early bitumen phase, Well GS18, 5177.82 m. **(H)** Silicified matrix dolomite (MD) predate early bitumen phase and MVT minerals (pyrite and fluorite), Well MX51, 5383.48 m. **(I)** Coexisting relationship between sphalerite and late quartz phase characterized by growth zone, Well GS109, 5317.4 m.

syndiagenetic stage, the carbonate sediments have not completed the mineral stabilization process, and the mineral components with unstable chemical properties are selectively dissolved by meteoric freshwater, resulting in the formation of secondary reservoir spaces. Meanwhile, microbial dolomitization has limited increase in reservoir porosity, but it can increase the anti-compaction ability, which is of great significance to the preservation of reservoir spaces. Silicification is the most unfavorable for reservoir formation in the syndiagenetic stage. The average porosity of the silified MD is 0.22% lower than the MD (the median decreased by 0.20%), and the average permeability is decreased by 0.220 mD (the median decreased by 0.002 mD) (Figure 10). After silicification in the syndiagenetic stage, the mineral composition of the MD changed from magnesium calcium carbonate to silica, and the later constructive diagenetic alterations were almost ineffective (Figure 2D). Fortunately, the duration and influence range of silicification in the syndiagenetic stage are very limited and will not cause large-scale destructive effects. The Ediacaran is a period of major plate tectonic recombination and extensive non-orogenic volcanic activity (Chen et al., 2009). It is presumed that submarine volcanic activity provides silicon-rich hydrothermal fluids for silicification at the syndiagenetic stage (Ma et al., 2014).

With the increase of buried depth, the Dengying Formation gradually entered the early diagenetic stage. Zhou et al. (2020) proposed that diagenesis in the early diagenetic stage is not conducive to the preservation of reservoir spaces in the Dengying Formation. After this stage, the porosity of dolomite reservoir in the Dengying Formation decreases to below 5%.

The tectonic uplift caused by Tongwan Movement led the Dengying Formation to enter the epidiagenetic stage (Figure 8A). At this stage, the interior and top of the Dengying Formation are generally eroded to varying degrees, forming a large number of non-fabric selective karst pores (Figure 9A), fissures (Figure 9B), and vugs (Figure 9C). Within these secondary reservoir spaces, typical marks of epidiagenetc stage, such as vadose silts, are observed (Figure 9D). After this stage, the average porosity increased by 1.51% (median increased by 1.36%), and the average permeability increased by 0.611 mD (median increased by 0.033mD) (Figure 10). However, because the fractures and vugs of the drilling cores are very developed (Figure 2), the plunger samples for measurement cannot reflect the real reservoir physical properties, and the actual increment of porosity and permeability far exceeds the measured data. Therefore, some scholars have proposed that the total porosity of the Dengying Formation reservoir increased by 10%–20% during epidiagenetic stage (Zhou et al., 2020).

With the end of Tongwan movement, the sea level rose again, and the reservoir space of the Dengying Formation experienced the marine flooding (Ding et al., 2019). The FD precipitated directly from the seawater filling the reservoir spaces along the inner walls (Figures 9B,C). In the second-time early diagenetic stage, the MCD cement directly precipitated from the altered seawater continues to fill the remaining reservoir spaces.

With the increase of burial depth, the Dengying Formation enters middle diagenetic stage. During this period, two stages of hydrothermal alterations occurred, corresponding to Late Silurian to Devonian and Late Permian, respectively. Significant differences in the alteration effects of hydrothermal fluids on MD and karstified MD are revealed. Under the first-stage hydrothermal alteration, the MD recrystallized to form FMD rich in intercrystalline pores. This process increases the average porosity by 1.64% (median increased by 1.28%) and the average permeability by 0.226 mD (median increased by 0.002 mD) (Figure 10). On the other hand, under the action of the first-stage hydrothermal activity, the MD underwent dilational

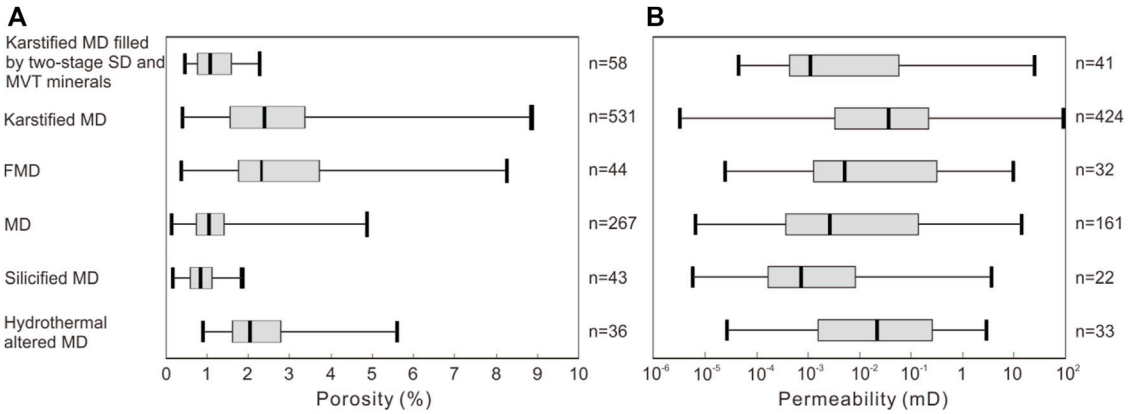

FIGURE 10
(A) Boxplot of porosity distribution in different rock fabrics of the Dengying Formation, Central Sichuan Basin. **(B)** Boxplot of permeablity distribution in different rock fabrics of the Dengying Formation, Central Sichuan Basin.

fracturing and dissolution, accompanied by subsequent precipitation of the first-stage SD cement. The second-stage hydrothermal activity did not lead to the recrystallization of the MD, but only showed dissolution and filling. The filling minerals not only had the second-stage SD cement, but also had MVT minerals such as pyrite, galena, quartz and sphalerite. After two-episode hydrothermal alterations, the average porosity of the MD increased by 1.15% (median increased by 1.01%) and the average permeability decreased by 0.135 mD (median increased by 0.019 mD) (Figure 10). In terms of the karstified MD, both hydrothermal alterations were destructive (Figure 9), resulting in an average porosity decrease of 1.44% (median decreased by 1.32%) and an average permeability decrease of 0.139 mD (median decreased by 0.036 mD) (Figure 10). As mentioned above, since karstified MD samples are all core plunger samples, the actual damage of reservoir physical properties caused by hydrothermal alteration is much worse.

6 Conclusions

1) Two phases of dolomite and three phases of dolomite cement are distinguished in the Ediacaran Dengying Formation deep dolomite reservoirs of Central Sichuan Basin as follows: (1) matrix dolomites (MD), (2) fine-medium crystalline dolomites (FMD), (3) fibrous dolomites (FD), (4) medium-coarse crystalline dolomites (MCD), and (5) saddle dolomite (SD). The FMD is the product of the recrystallization of MD caused by the first hydrothermal fluid during middle diagenetic stage. The FD is derived from marine flooding of the karst system during epidiagenetic stage. The MCD is derived from modified coeval seawater during the second-time early diagenetic stage. The early SD phase is precipitated during the Late Silurian to Devonian, when the Dengying Formation was in the middle diagenetic stage. The late SD phase is precipitated during the Late Permian, while the Dengying Formation is still in the middle diagenetic stage.
2) Syndiagenetic microbial dolomitization has limited increase in reservoir porosity, but it is of great significance to the reservoir space preservation. Syndiagenetic silicification is the most unfavorable for reservoir formation, but it will not cause large-scale destructive effects. Epidiagenetic stage trigger great increase of physical properties of the Dengying Formation dolomite reservoir. Two-stage early diagenetic stages are both destructive to reservoir space maintenance. During middle diagenetic stage, two-stage of hydrothermal alterations occurred, corresponding to Late Silurian to Devonian and Late Permian, respectively. Hydrothermal alteration of the MD is both constructive and destructive, but overall it is constructive, but the improvement of physical properties is limited. Two-stage hydrothermal alterations lead to damage of reservoir physical properties for the karstified MD.

Data availability statement

The raw data supporting the conclusions of this article will be made available by the authors, without undue reservation.

Author contributions

YG contributed as the major author of the article. CY and ML conceived the project. HW, LZ, and YJ collected the samples. ZW and XL analyzed the samples. All authors contributed to the article and approved the submitted version.

Funding

This study was funded by the National Natural Science Foundation of China (Grant No. 41972165) and National Natural Science Foundation of China (Grant No. 42202166).

Conflict of interest

Authors CY and ML were employed by the company PetroChina Southwest Oil and Gas Field Company.

The remaining authors declare that the research was conducted in the absence of any commercial or financial relationships that could be construed as a potential conflict of interest.

Publisher's note

References

Burns, S. J., Haudenschild, U., and Matter, A. (1994). The strontium isotopic composition of carbonates from the late Precambrian (560–540 Ma) Huqf Group of Oman. *Chem. Geol.* 111 (1-4), 269–282. doi:10.1016/0009-2541(94)90094-9

Chen, D., Wang, J., Qing, H., Yan, D., and Li, R. (2009). Hydrothermal venting activities in the early cambrian, south China: Petrological, geochronological and stable isotopic constraints. *Chem. Geol.* 258 (3-4), 168–181. doi:10.1016/j.chemgeo.2008.10.016

Ding, Y., Chen, D., Zhou, X., Guo, C., Huang, T., and Zhang, G. (2019). Cavity-filling dolomite speleothems and submarine cements in the Ediacaran Dengying microbialites, South China: Responses to high-frequency sea-level fluctuations in an "aragonite-dolomite sea". *Sedimentology* 66 (6), 2511–2537. doi:10.1111/sed.12605

Ding, Y., Li, Z., Liu, S., Song, J., Chen, D., Sun, W., et al. (2021). Sequence stratigraphy and tectono-depositional evolution of a late Ediacaran epeiric platform in the upper Yangtze area, South China. *Precambrian Res.* 354, 106077. doi:10.1016/j.precamres.2020.106077

Dorobek, S. L. (1987). Petrography, geochemistry, and origin of burial diagenetic facies, Siluro-Devonian Helderberg group (Carbonate rocks), central Appalachians. *Am. Assoc. Pet. Geol. Bull.* 71 (5), 492–514. doi:10.1306/94886EDE-1704-11D7-8645000102C1865D

Du, Y., Fan, T., Machel, H. G., and Gao, Z. (2018). Genesis of upper cambrian-lower ordovician dolomites in the tahe oilfield, Tarim Basin, NW China: Several limitations from petrology, geochemistry, and fluid inclusions. *Mar. Petroleum Geol.* 91, 43–70. doi:10.1016/j.marpetgeo.2017.12.023

Ehrenberg, S. N., Nadeau, P. H., and Steen, O. (2009). Petroleum reservoir porosity versus depth: Influence of geological age. *Am. Assoc. Pet. Geol. Bull.* 93 (10), 1281–1296. doi:10.1306/06120908163

Fairchild, J., and Spiro, B. (1987). Petrological and isotopic implications of some contrasting Late Precambrian carbonates, NE Spitsbergen. *Sedimentology* 34 (6), 973–989. doi:10.1111/j.1365-3091.1987.tb00587.x

Feng, M. Y., Wu, P. C., Qiang, Z. T., Liu, X. H., Duan, Y., and Xia, M. L. (2017). Hydrothermal dolomite reservoir in the Precambrian dengying formation of central Sichuan basin, Southwestern China. *Mar. Petroleum Geol.* 82, 206–219. doi:10.1016/j.marpetgeo.2017.02.008

Gu, Y., Jiang, Y., Lei, X., Chen, Z., Zhou, L., Fu, Y., et al. (2021). The major controlling factors and different oolitic shoal reservoir characteristics of the Triassic Feixianguan Formation, Eastern LonggangArea, NE Sichuan Basin, SW China. *Acta Geol. sinica-. Engl. Ed.* 95 (3), 895–908. doi:10.1111/1755-6724.14672

Gu, Y., Jiang, Y., Qing, H., Feng, L., Feng, L., Fu, Y., et al. (2020). Reservoir characteristics, pore structure, and main controlling factors of oolitic shoal reservoir in feixianguan formation: A case study from eastern kaijiang-liangping trough. *Arab. J. Geosci.* 13, 309. doi:10.1007/s12517-020-05286-x

Gu, Y., Zhou, L., Jiang, Y., Jiang, C., Luo, M., and Zhu, X. (2019). A model of hydrothermal dolomite reservoir facies in Precambrian dolomite, Central Sichuan Basin, SW China and its geochemical characteristics. *Acta Geol. sinica-. Engl. Ed.* 93 (1), 130–145. doi:10.1111/1755-6724.13770

Guo, C., Chen, D., Qing, H., Dong, S., Li, G., Wang, D., et al. (2016). Multiple dolomitization and later hydrothermal alteration on the Upper Cambrian-Lower Ordovician carbonates in the northern Tarim Basin, China. *Mar. Petroleum Geol.* 72, 295–316. doi:10.1016/j.marpetgeo.2016.01.023

He, Z., Ma, Y., Zhu, D., Duan, T., Geng, J., Zhang, J., et al. (2021). Theoretical and technological progress and research direction of deep and ultra-deep carbonate reservoirs. *Oil Gas Geol.* 42 (3), 533–546. doi:10.11743/ogg20210301

Huang, H., Huyskens, M. H., Yin, Q., Cawood, P. A., Hou, M., Yang, J., et al. (2022). Eruptive tempo of Emeishan large igneous province, southwestern China and northern Vietnam: Relations to biotic crises and paleoclimate changes around the Guadalupian-Lopingian boundary. *Geology* 50 (9), 1083–1087. doi:10.1130/G50183.1

Jiang, Y., Gu, Y., Li, K., Li, S., Luo, M., and He, B. (2018). Space types and origins of hydrothermal dolomite reservoirs in the Middle Permian strata, Central Sichuan Basin. *Nat. Gas. Ind.* 38 (2), 16–24. doi:10.3787/j.issn.1000-0976.2018.02.003

Jiang, Y., Gu, Y., Liu, F., Liu, D., Chen, W., Liao, Y., et al. (2017). Discovery and exploration significance of Permian-Triassic trough and platforrrn margin facies in Zhongxian-Yuchi area, eastern Sichuan Basin. *Acta Pet. Sin.* 38 (12), 1343–1355. doi:10.7623/syxb201712

Jiang, Y., Tao, Y., Gu, Y., Wang, J., Qiang, Z., Jiang, N., et al. (2016). Hydrothermal dolomitization in Dengying Formation, gaoshiti-moxi area, Sichuan Basin, SW China. *Petroleum Explor. Dev.* 43 (1), 54–64. doi:10.1016/S1876-3804(16)30006-4

Land, L. S. (1983). "The application of stable isotopes to studies of the origin of dolomite and to problems of diagenesis of clastic sediments," in *Stable isotopes in sedimentary Geology, SEPM short course*. Editors M. A. Arthur, T. F. Anderson, I. R. Kaplan, J. Veizer, and L. S. Land (Tulsa, Oklahoma, 4.1–4.22.

Li, H. (2022). Research progress on evaluation methods and factors influencing shale brittleness: A review. *Energy Rep.* 8, 4344–4358. doi:10.1016/j.egyr.2022.03.120

Li H., H., Zhou, J., Mou, X., Guo, H., Wang, X., An, H., et al. (2022). Pore structure and fractal characteristics of the marine shale of the longmaxi formation in the changning area, southern Sichuan Basin, China. *Front. Earth Sci.* 10, 1018274. doi:10.3389/feart.2022.1018274

Li, J., Bai, B., Bai, Y., Lu, X., Zhang, B., Qin, S., et al. (2022a). Fluid evolution and hydrocarbon accumulation model of ultra-deep gas reservoirs in Permian Qixia Formation of northwest Sichuan Basin, SW China. *Petroleum Explor. Dev.* 49 (4), 719–730. doi:10.1016/s1876-3804(22)60305-7

Li, J., Li, H., Yang, C., Wu, Y. J., Gao, Z., and Jiang, S. L. (2022b). Geological characteristics and controlling factors of deep shale gas enrichment of the Wufeng-Longmaxi Formation in the southern Sichuan Basin, China. *Lithosphere* 2022 (12), 4737801. doi:10.2113/2022/4737801

Lin, X., Peng, J., Hou, Z., Han, H., Li, X., and Ma, C. (2018). Study on characteristics and geneses of algal dolostone of the upper sinian Dengying Formation in the hanyuan-ebian area of sichuan province, China. *Acta Sedimentol. Sin.* 36 (1), 57–71. doi:10.3969/j.issn.1000-0550.2018.008

Liu, S., Huang, W., Jansa, L. F., Wang, G., Song, G., Zhang, C., et al. (2014). Hydrothermal dolomite in the upper sinian (upper proterozoic Dengying Formation, east Sichuan Basin, China. *Acta Geol. Sin. - Engl. Ed.* 88 (5), 1466–1487. doi:10.1111/1755-6724.12312

Liu, W., Qiu, N. S., Xu, Q. C., and Chang, J. (2018b). The quantitative evaluation of the pressurization caused by hydrocarbon generation in the Cambrian Qiongzhusi Formation of the Gaoshiti-Moxi area, Sichuan Basin. *Petroleum Sci. Bull.* 3 (3), 262–271. doi:10.3969/j.issn.2096-1693.2018.03.024

Liu, W., Qiu, N., Xu, Q., and Liu, Y. (2018a). Precambrian temperature and pressure system of Gaoshiti-Moxi block in the central paleo-uplift of Sichuan Basin, southwest China. *Precambrian Res.* 313, 91–108. doi:10.1016/j.precamres.2018.05.028

Ma, W., Liu, S., Huang, W., Chen, C., and Zhang, C. (2014). Fabric characteristics and formation mechanism of chert in sinian Dengying Formation, eastern chongqing. *Acta Geol. Sin.* 88 (2), 239–253. doi:10.3969/j.issn.0001-5717.2014.02.007

Meng, F., Ni, P., Schiffbauer, J. D., Yuan, X., Zhou, C., Wang, Y., et al. (2011). Ediacaranseawater temperature: Evidence from inclusions of sinian halite. *Precambrian Res.* 184 (1-4), 63–69. doi:10.1016/j.precamres.2010.10.004

Peng, B., Li, Z., Li, G., Liu, C., Zhu, S., Zhang, W., et al. (2018). Multiple dolomitization and fluid flow events in the precambrian Dengying Formation of Sichuan Basin, southwestern China. *Acta Geol. Sin. - Engl. Ed.* 92 (1), 311–332. doi:10.1111/1755-6724.13507

Peng, J., Zhang, H., and Lin, X. (2018). Study on characteristics and Genesis of botryoidal dolostone of the upper sinian Dengying Formation: A case study from hanyuan region, sichuan. China. *Carbonates Evaporites* 33, 285–299. doi:10.1007/s13146-017-0343-8

Qi, L., Gu, Y., He, P., Wang, Z., Jiang, Y., Li, S., et al. (2021). Hydrothermal dolomitization in the middle permian in the central Sichuan Basin, SW China: Evidence from petrology, geochemistry, and fluid inclusions. *Arab. J. Geosci.* 14, 55. doi:10.1007/s12517-020-06386-4

Roberts, N. M. W., Rasbury, E. T., Parrish, R. R., Smith, C. J., Horstwood, M. S. A., and Condon, D. J. (2017). A calcite reference material for LA-ICP-MS U-Pb geochronology. *Geochem. Geophys. Geosyst.* 18 (7), 2807–2814. doi:10.1002/2016GC006784

Schmoker, J. W., and Hally, R. B. (1982). Carbonate porosity versus depth:A predictable relation for South Florida. *AAPG Bull.* 66 (12), 2561–2570.

Shahida, W., Naila, S., and Yasir, F. (2013). Rare Earth and high field-strength elements in the multani mitti clay: A study using inaa. *Geostand. Geoanal. Res.* 37 (2), 197–205. doi:10.1111/j.1751-908X.2012.00186.x

Shi, Z., Wang, Y., Tian, Y., and Wang, C. (2013). Cementation and diagenetic fluid of algal dolomites in the sinian Dengying Formation in southeastern Sichuan Basin. *Sci. China Earth Sci.* 56 (2), 192–202. doi:10.1007/s11430-012-4541-x

Su, A., Chen, H., Feng, Y., Zhao, J., Wang, Z., Hu, M., et al. (2022). *In situ* U-Pb dating and geochemical characterization of multi-stage dolomite cementation in the Ediacaran Dengying Formation, Central Sichuan Basin, China: Constraints on diagenetic, hydrothermal and paleo-oil filling events. *Precambrian Res.* 368, 106481. doi:10.1016/j.precamres.2021.106481

Tang, T., Xue, Y., and Yu, C. (1980). The characters and environment significance of the Sinian algae-carbonates in the southern part of China. *Chin. Sci. Bull.* 32 (18), 853–855. CNKI:SUN:KXTB.0.1980-18-010.

Wang, G., Liu, S., Li, N., Wang, D., and Gao, Y. (2014). Formation and preservation mechanism of high quality reservoir in deep burial dolomite in the Dengying Formation on the northern margin of the Sichuan Basin. *Acta Petrol. Sin.* 30 (3), 667–678. doi:10.1134/S1075701514020044

Wang, Z., Jiang, C., Jiang, Y., Zhang, J., and Gu, Y. (2018). Distribution patterns and controlling factors for reservoir characteristic difference of oolitic shoals, Feixian'guan Formation, eastern Longgang area, SW China. *Arab. J. Geosci.* 11, 751. doi:10.1007/s12517-018-4082-5

Xu, F., Xu, G., Liang, J., Yuan, H., Liu, Y., and Xu, F. (2016). Multi-stage fluid charging and critical period of hydrocarbon accumulation of the Sinian Dengying Formation in central Sichuan Basin. *Acta Geol. Sin. Engl. Ed.* 90 (4), 1549–1550. CNKI:SUN:DZXW.0.2016-04-034.

Zhao, W., Shen, A., Zheng, J., Qiao, Z., Pan, L., Hu, A., et al. (2018). Genetic types and distinguished characteristics of dolomite and the origin of dolomite reservoirs. *Petroleum Explor. Dev.* 45 (6), 983–997. doi:10.1016/s1876-3804(18)30103-4

Zhao, W., Shen, A., Zheng, J., Qiao, Z., Wang, X., and Lu, J. (2014). The porosity origin of dolostone reservoirs in the Tarim, Sichuan and Ordos basins and its implication to reservoir prediction. *Sci. China Earth Sci.* 44 (9), 2498–2511. doi:10.1007/s11430-014-4920-6

Zhao, W., Xie, Z., Wang, X., Shen, A., Wei, G., Wang, Z., et al. (2021). Sinian gas sources and effectiveness of primary gas-bearing system in Sichuan Basin, SW China. *Petroleum Explor. Dev.* 48 (6), 1260–1270. doi:10.1016/s1876-3804(21)60285-9

Zhou, Y., Jiang, Y., Liang, J., Gu, Y., Fu, Y., and Xiao, Y. (2020). Characteristics and controlling factors of dolomite karst reservoirs of the Sinian Dengying Formation, central Sichuan Basin, southwestern China. *Precambrian Res.* 343, 105708. doi:10.1016/j.precamres.2020.105708

Zhou, Y., Yang, F., Ji, Y., Zhou, X., Zhang, C., and Xiao, Y. (2021). Reservoir characteristics and major controlling factors of the cambrian xixiangchi formation, central Sichuan Basin, southwest China. *J. Energy Eng.* 147 (6), 04021051. doi:10.1061/(ASCE)EY.1943-7897.0000803

Zhou, Z., Wang, X., Yin, G., Yuan, S., and Zeng, S. (2016). Characteristics and Genesis of the (sinian) Dengying Formation reservoir in central sichuan, China. *J. Nat. Gas Sci. Eng.* 29, 311–321. doi:10.1016/j.jngse.2015.12.005

Zhu, D., Zhang, D., Zhang, R., Feng, J., and He, Z. (2015). Fluid alteration mechanism of dolomite reservoirs in Dengying Formation, South China. *Acta Pet. Sin.* 36 (10), 1188–1198. doi:10.7623/syxb201510002100

Zhu, X., Gu, Y., Jiang, Y., Tang, T., Xu, W., Li, K., et al. (2019). Characteristic and reservoir body classification & evaluation of Sinian Dengying karst reservoirs in the Gaoshiti Block of central Sichuan Basin. *Nat. Gas. Ind.* 39 (3), 38–46. doi:10.3787/j.issn.1000-0976.2019.03.005

Zou, C., Xu, C., Wang, Z., Hu, S., Yang, G., Li, J., et al. (2011). Geological characteristics and forming conditions of the large platform margin reef-shoal gas province in the Sichuan Basin. *Petroleum Explor. Dev.* 38 (6), 641–651. CNKI:SUN:SKYK.0.2011-06-002.